

Existence of traversable wormholes in the spherical stellar systems

A. Övgün* and M. Halilsoy†

*Physics Department, Eastern Mediterranean University,
Famagusta, Northern Cyprus, Mersin 10, Turkey.*

(Dated: May 30, 2016)

Potentiality of the presence of traversable wormholes in the outer/inner regions of the halos of galaxies, situated on the Navarro-Frenk-White (NFW) density profile and Universal Rotation Curve (URC) dark matter models have been investigated recently [27–29, 49–52]. Since this covers our own galaxy also as a possible home for traversable wormholes it prompts us to further the subject by considering alternative density distributions. From this token herein we make use of the Einasto model [12, 13, 35] to describe the density profiles for the same purpose. Our choice for the latter is based on the fact that theoretical dark matter halos produced in computer simulations are best described by such a profile. For technical reasons we trim the number of parameters in the Einasto profile to a possible minimum. Based on such a model it is shown that traversable wormholes in the outer regions of spiral galaxies are possible while the inner part regions prohibit such formations.

Keywords: wormholes, Milky Way, spherical stellar systems, galaxies, halos, dark matter

I. INTRODUCTION

Although Flamm’s work on the wormhole physics dates back to 1916, in connection with the newly found Schwarzschild solution [18], wormhole solutions were firstly considered from physics standpoint by Einstein and Rosen (ER) in 1935, which is known today as Einstein-Rosen bridge connecting two identical space-times [14]. Then in 1955 Wheeler used ”geons” (self-gravitating bundles of electromagnetic fields) by giving the first diagram of a doubly-connected-space [58]. Wheeler added the term ”wormhole” to the physics literature, however he defined it at the quantum scale. After that, first traversable wormhole was proposed by Morris-Thorne in 1988 [36]. Then Morris, Thorne, and Yurtsever investigated the requirements of the energy condition for wormholes [37]. After while, Visser constructed a technical way to make thin-shell wormholes which thoroughly surveyed the research landscape as of 1988 [47, 61–63]. After this, there are many papers written to support this idea [22, 33, 34, 43].

In 1933 F. Zwicky, was the first astronomer to propose the existence of the dark matter (DM) after that he observed the motions of the galaxies in the Coma Cluster, a galaxy cluster roughly 320 million light-years away and nearly 2 light-years across, and found that it moved too rapidly [65]. He noted that its speed of revolution, which depends on the weight and position of the objects inside, implied the cluster had much more mass than he could see. He decided there must be a hidden ingredient, known as dark matter, that caused the motions of these galaxies to be so large. In 1978, American astronomer Vera Rubin looked at individual galaxies and she realized that the outer stars were spinning as quickly as the interior stars, and sometimes faster [59]. It is concluded that the galaxies must be surrounded by a halo of matter which is not seen. Theorists have postulated many candidates for what DM might be. But the most widely accepted hypothesis is the weakly interacting massive particles (WIMPs), a particle that interacts with gravity but not light, hence its invisibility to us [7]. Neither WIMPs nor any other particle that could successfully explain DM exist in the standard model of particle physics, the theoretical framework that has successfully predicted nearly all the phenomena in the universe. Thus, the identity of the DM particle remains one of the outstanding mysteries in particle physics and cosmology. According to the latest results from the Planck satellite [46], a mere 26.8% DM percent of the universe which plays a central role in modeling of cosmic structure, galaxy formation and evolution and on explanations of the anisotropies observed in the cosmic microwave background (CMB), 4.9% is made of ordinary matter which is matter composed of atoms or their constituents and 68.3% is dark energy (DE) that tends to accelerate the expansion of the universe [8, 20, 21]. Certain types of DM can actually help the formation of wormholes. For example, dissipative DM in which DM particles forming galactic halos are presumed to have dissipative self-interactions can aid the formation of black holes by dissipative collapse, and subsequent to wormholes. Now, in this types of models one can consider either DM collapsed to a disk, or a quasi-isothermal profile [16, 17, 19, 26, 38].

*Electronic address: ali.ovgun@emu.edu.tr

†Electronic address: mustafa.halilsoy@emu.edu.tr

Recently, Rahaman et al. have used both the NFW [41, 51, 52]

$$\rho(r) = \frac{\rho_s}{\frac{r}{r_s} \left(1 + \frac{r}{r_s}\right)^2}, \quad (1)$$

and URC DM density profiles [4]

$$\rho(r) = \frac{\rho_0 r_0^3}{(r + r_0)(r^2 + r_0^2)} \quad (2)$$

where ρ_0 , ρ_s , r_0 and r_s are all constants, to show the potentiality of the presence of traversable wormholes in the outer and the inner part, respectively, of the halo.

In this paper, following similar line of thought, we study the Einasto model [12, 13, 35] which is the special function that arranges the finest total fit to the halo density profiles. It tells how the density ρ of a spherical stellar system changes with distance r from its center [23]: This is expressed by the density profile

$$\rho(r) \propto e^{-Ar^\alpha} \quad (3)$$

with constants A and α .

The bounded parameter α which is called Einasto index, adjusts the degree of curvature of the profile [9, 53]

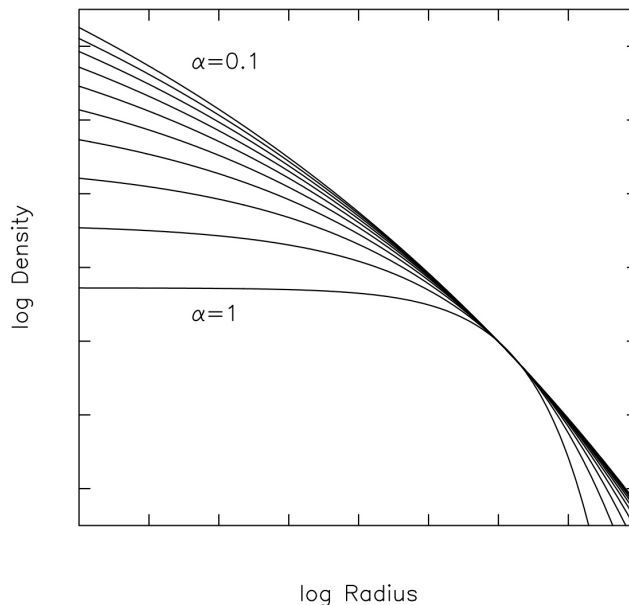


FIG. 1: Einasto profile in log-log plot (the parameter α controls the degree of curvature of the profile) from Eqn. 3 .

$$\rho(r) = \rho_0 \exp \left[-\frac{2}{\alpha} \left(\left(\frac{r}{r_0} \right)^\alpha - 1 \right) \right]. \quad (4)$$

simply named as the Einasto model in the present paper which is plotted in Fig. 1. For the Milky Way galaxy, we have $r_0 = 9.11$ kpc and $\rho_0 = 5 \times 10^{-24} (r_0/8.6 \text{ kpc})^{-1} \text{gcm}^{-3}$ [4, 32].

The slopes of the NFW profile has the range from the inner/outer ($r \rightarrow 0 / r \rightarrow \infty$) are depicted in Figs. 2 and 3 below. On the other hand, the values are different for the Einasto profile which are included as limiting cases of isothermal and Gaussian, ($\alpha = 0$, $\alpha = 2$, respectively). The difference between the Einasto and NFW profiles appears at small and large radial distances. After all, on scales of concern for gas or stellar dynamics and strong gravitational lensing the Einasto profile with $\alpha = 0.25$ is very akin to the NFW profile, and on scales of concern for weak gravitational lensing the Einasto profile with $\alpha = 0.2$ is quite similar to the NFW profile. Galaxy mass halos typically have $\alpha = 0.16$ as referred in Figs. 2 and 3 [10].

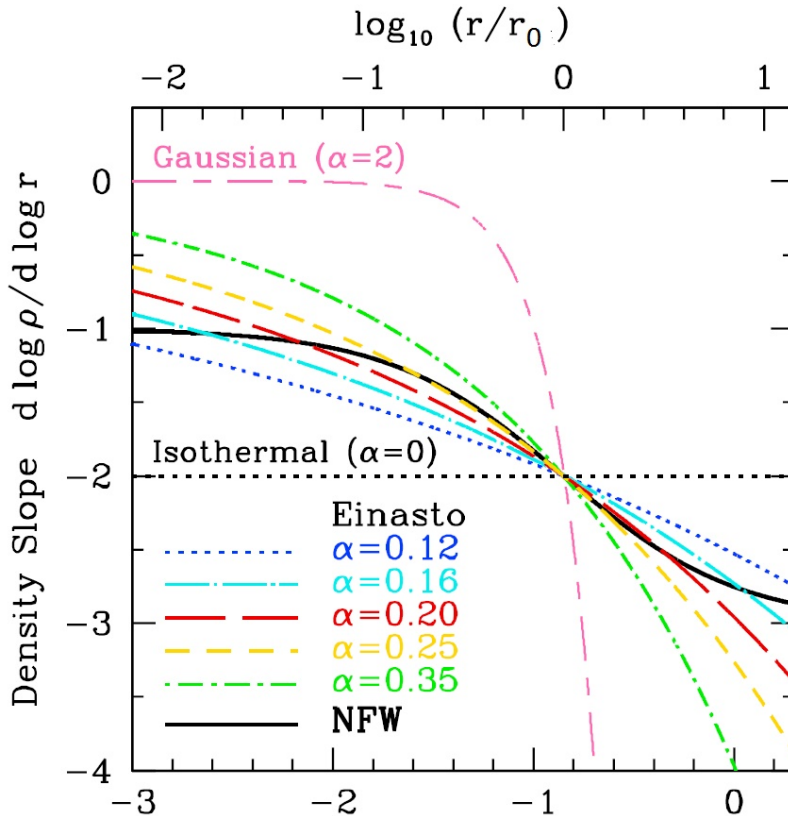


FIG. 2: Density profiles of Einasto and NFW, density slope ($d \log \rho / d \log r$), [10]

Einasto's model has been used in the description of many systems, such as galaxies, and halos. It is used to show the DM profiles of simulated halos as well as the NFW profile [2, 9, 55]. The Einasto profile has a finite (zero) central slope, in contrast to the NFW profile which has a divergent (infinite) central density. Due to the restricted resolution of N-body simulations, it is unclear yet which model description fit well to the central densities of simulated DM halo. The observations of both the Milky Way and some galaxies may be compatible with the NFW profile for the DM halo [24, 31, 40, 57, 60]. There are also self-interacting dark matter (SIDM) simulations and baryon feedback simulations [6, 11, 54]. The SIDM is attractive because it offers a means to lower the central densities of galaxies without destroying the successes of CDM on large scales. Cosmological simulations that contain only CDM indicate that DM haloes should be cuspy and with (high) concentrations that correlate with the collapse time of the halo. One possible answer is feedback in which the expulsion of gas from galaxies can result in lower DM densities compared to dissipationless simulations, and thus bring CDM models in line with observations [54, 64]. Furthermore baryon feedback has most significant effects on the inner density profiles which are typically shallower than isothermal and the halo concentrations tend to be lower than in the absence of baryons. For instance the strong feedback models reduce the baryon fraction in galaxies by a factor of 3 relative to the case with no feedback [6].

The DM profile of smaller galaxies tend to have flatter distributions of DM in the central region, known as the cuspy halo problem [44, 45]. Our purpose in this paper is to search for possible traversable wormholes in a spiral galaxy specified by the Einasto density profile. Wormholes are solutions to Einstein's equations that connect different universes or tunnels through different parts of the same universe. Our primary aim is to consider the Milky Way galaxy as a test bed for this venture. To this end we choose the parameter r_0 of Milky Way to coincide with the throat of the traversable wormhole whereas the second parameter α is in a restricted range. From the Einstein equations we derive the equations for the density and pressures in terms of the metric functions and their derivatives. Although our analytical functions are expressed in terms of the Whittaker functions [1] the detailed analysis are not imperative. It suffices for us to check the null-energy condition and satisfaction of the flare-out conditions [36, 37]. The same technical handicap prevents us to investigate the stability of the resulting traversable wormhole that may exist in the Milky Way galaxy. It is observed that at the central region Einasto profile does not give a traversable wormhole solution because violation of null energy condition is not satisfied there. But in the outward region we obtain possible

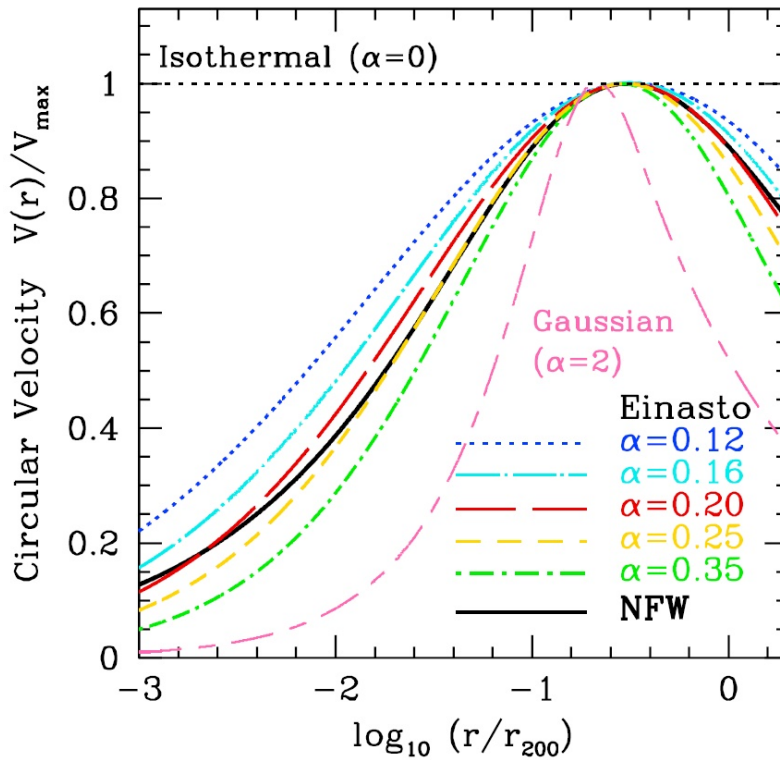


FIG. 3: Comparison of NFW (solid black lines) and Einasto (colored lines) profiles. In this example the halo concentration $c_{200} = 7.1$ [10]

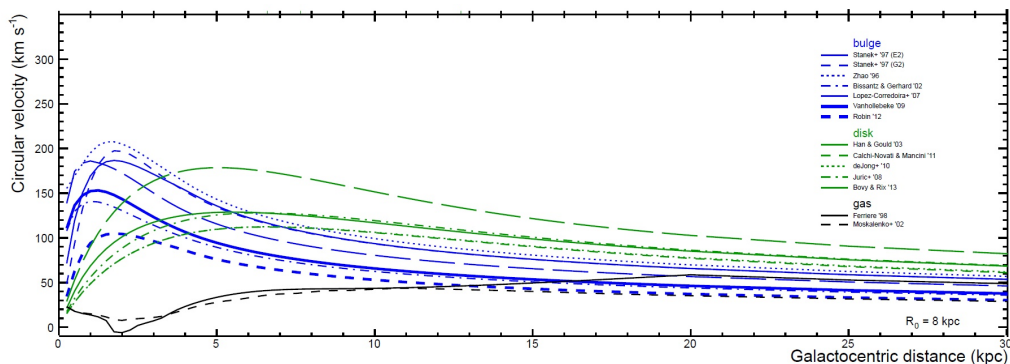


FIG. 4: Rotational velocity curve for Milkyway (the contribution to the rotation curve as predicted from different models for the stellar bulge (blue), stellar disk (green) and gas (black). We assume a distance to the galactic center $r_0 = 8$ kpc [24])

traversable wormholes.

The paper is organized as follows. In Sec. II we present the Einstein equations for wormhole space-time and we find their solutions under the Einasto DM profile. In Section III we discuss our results and conclude the paper.

II. TRAVERSABLE WORMHOLES UNDER THE EINASTO DM PROFILE

The spherically symmetric and static wormhole geometry which was proposed by Morris-Thorne is given by the line element [36]

$$ds^2 = -e^{2f(r)} dt^2 + \left(1 - \frac{b(r)}{r}\right)^{-1} dr^2 + r^2(d\theta^2 + \sin^2\theta d\phi^2), \quad (5)$$

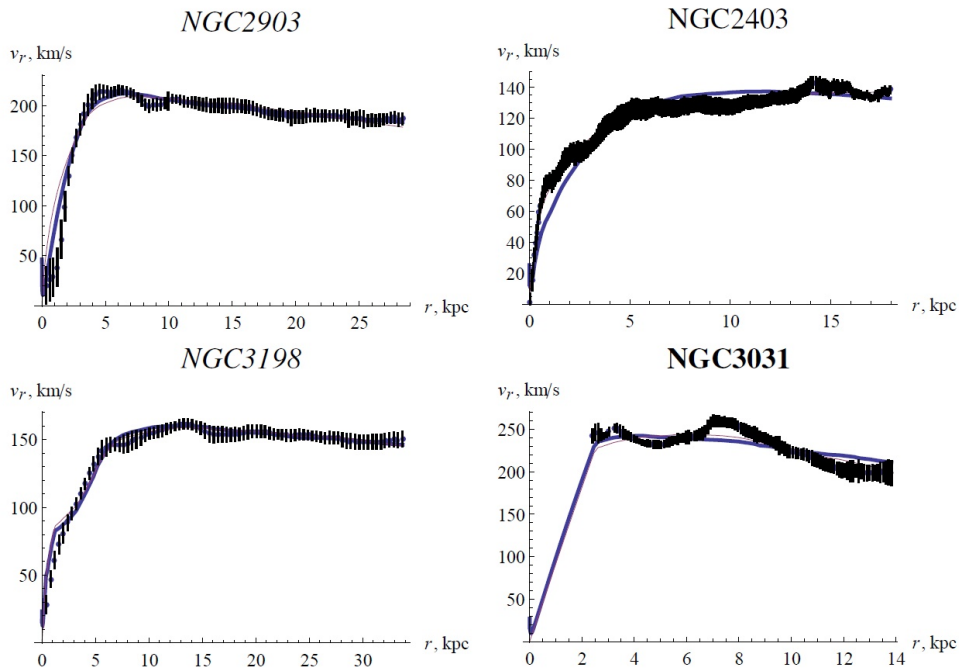


FIG. 5: Rotational curves $v(r)$ for some galaxies from THINGS survey together with fits. Blue thick curves show best fits by DM distributions of semi-degenerate configurations, while magenta thin curves show Einasto profile best fits [56]

where the function $b(r)$ defines the spatial shape function, and $f(r)$ stands for the redshift function. The radial coordinate r ranges from $+\infty$ to $b(r_0) = r_0$ (minimum radius condition that any wormhole must satisfy). The minimum value of the r is r_0 , called the throat of the wormhole. The proper radial distance is given by

$$l(r) = \pm \int_{r_0}^r \frac{dr}{\sqrt{\left(1 - \frac{b(r)}{r}\right)}}. \quad (6)$$

Properties of such traversable wormholes are listed below [36, 37];

- Spherically symmetric, static metric,
- Satisfy the Einstein field equations,
- No event horizon, i. e. $e^{f(r)} \neq 0$,
- "Throat" $r = r_0$ connects two asymptotically flat space-time regions, (for Milky Way galaxy $r_0 = 9.11$ kpc)
- The stress-energy tensor (violating the null-energy condition (NEC) with $\rho + p_r < 0$, where ρ is the energy density and p_r the radial pressure),
- Physically reasonable construction materials, (for Milky Way galaxy $\rho_0 = 5 \times 10^{-24} (r_0/8.6 \text{ kpc})^{-1} \text{ g cm}^{-3}$)
- Bearable tidal gravitational forces,
- Satisfy the flare-out condition at the throat ($b'(r_{th}) < 1$), while $b(r) < r$ near the throat,
- Finite and reasonable crossing time,
- Stable against perturbations.

The Einstein field equation are given by

$$G_{\nu}^{\mu} = 8\pi T_{\nu}^{\mu} \quad (7)$$

where T_ν^μ is the stress-energy tensor, G_ν^μ is the Einstein tensor with the units in which $c = G = 1$. Field equations relate space-time curvature to matter and energy distribution. The non-zero G_ν^μ components are

$$G_t^t = -\frac{b'}{r^2}, \quad (8)$$

$$G_r^r = \frac{-b}{r^3} + 2\left(1 - \frac{b}{r}\right)\frac{f'}{r}, \quad (9)$$

$$G_\theta^\theta = G_\phi^\phi = \left(1 - \frac{b}{r}\right) \left[f'' + f'^2 + \frac{f'}{r} - \left(f' + \frac{1}{r}\right) \left\{ \frac{b'r - b}{2r(r-b)} \right\} \right], \quad (10)$$

in which a prime is $\frac{d}{dr}$.

It is assumed that DM is expressed in the form of general anisotropic energy-momentum tensor [3, 50], as follows

$$T_\nu^\mu = (\rho + p_r)u^\mu u_\nu + p_r g_\nu^\mu + (p_t - p_r)\eta^\mu \eta_\nu, \quad (11)$$

in which $u^\mu u_\mu = -\frac{1}{2}\eta^\mu \eta_\mu = -1$, and where p_t is the transverse pressure, p_r is the radial pressure and ρ is the energy density. A possible set of u^μ and η^μ are given by $u^\mu = (e^{2f(r)}, 0, 0, 0)$ and $\eta^\mu = (0, 0, \frac{1}{r}, \frac{1}{r \sin \theta})$. Let us add that once we restrict ourselves entirely to a collisionless cold DM the pressure terms should not be taken into account. Our choice implies accordingly that we aim a more general anisotropic fluid, at least for our future interest. The only non-zero components of T_ν^μ are

$$T_t^t = -\rho, \quad (12)$$

$$T_r^r = p_r, \quad (13)$$

$$T_\theta^\theta = T_\phi^\phi = p_t. \quad (14)$$

Furthermore we need to impose some constraints in order to solve Einstein field equations. One of them is the tangential velocity, (for a justification of this condition we refer to the book by Chandrasekhar [5, 30])

$$v^\phi = \sqrt{r f'} \quad (15)$$

which is responsible to fit the flat rotational curve for the DM. Other one is proposed by Rahaman et. al [50] that the observed rotational curve profile in the DM region is given by

$$v^\phi = \alpha r \exp(-k_1 r) + \beta [1 - \exp(-k_2 r)] \quad (16)$$

in which α , β , k_1 , and k_2 are constant positive parameters. It is illustrated in Fig.6. With this choice it is guaranteed that for $r \rightarrow \infty$ we obtain $v^\phi = \beta = \text{constant}$ which is required for flat rotation curves.

From the Eqns.(15) and (16), one obtains the redshift function as follows

$$f(r) = -\frac{\alpha^2 r}{2k_1 e^{(2k_1 r)}} - \frac{\alpha^2}{4k_1^2 e^{(2k_1 r)}} - \frac{2\alpha\beta}{k_1 e^{(k_1 r)}} + \frac{2\alpha\beta e^{(-k_1 r - k_2 r)}}{k_1 + k_2} + \beta^2 \ln(r) + 2\beta^2 E_i(1, k_2 r) - \beta^2 E_i(1, 2k_2 r) + D. \quad (17)$$

with the exponential integral E_i [25] and integration constant D . For large r , it is required also that $e^{2f(r)} = B_0 r^{(4v^\phi)}$ [5, 39, 48].

By using the Eqns. (15) and (16) and the Einasto density profile (Eqn. (4)), the Einstein field equations give us the tedious form of the shape function

$$b(r) = \frac{2^{(3-\frac{3}{\alpha})} \pi \rho_0}{\alpha} \exp\left(\frac{2}{\alpha}\right) \left(\frac{(r/r_0)^\alpha r^{-\alpha}}{\alpha}\right)^{-3/\alpha} \left[\left(\frac{1}{3(\alpha+3)(2\alpha+3)}\right) \alpha^3 r^{3(3/\alpha-1-(\alpha+3)/2\alpha)} \left(\frac{(r/r_0)^\alpha r^{-\alpha}}{\alpha}\right)^{3/\alpha}\right] \quad (18)$$

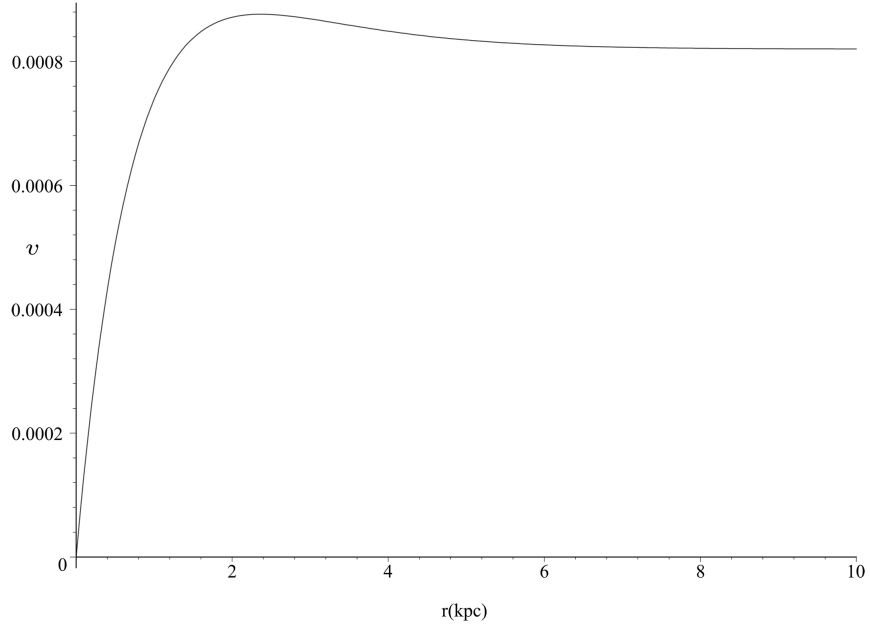


FIG. 6: Proposed rotational velocity with values of the parameters as $k_1 = k_2 = 1, \alpha = 0.0006$ and $\beta = 0.00082$ [50]

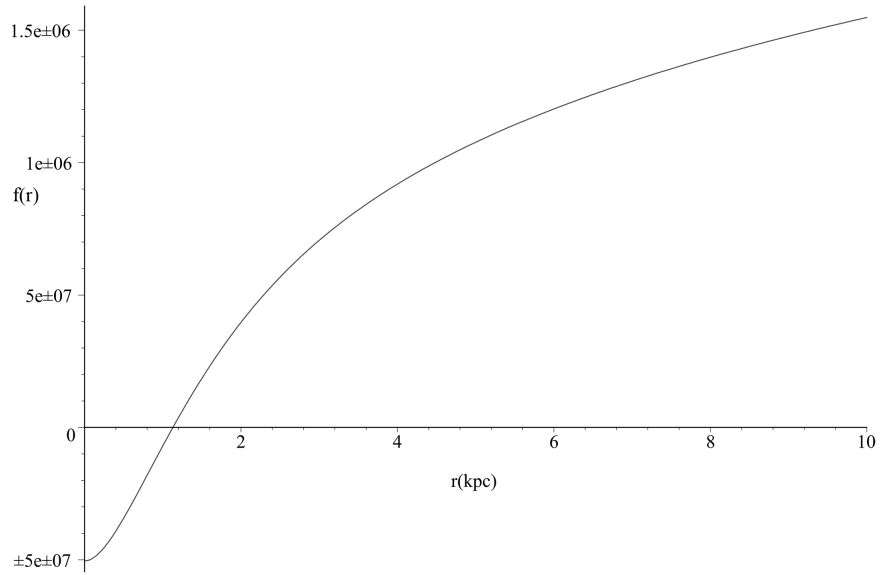


FIG. 7: $f(r)$ versus r ($k_1 = k_2 = 1, \alpha = 0.0006$ and $\beta = 0.00082$ [50])

$$\times \left(2\left(\frac{r}{r_0}\right)^\alpha + \alpha + 3 \right) \left(\frac{r}{r_0}\right)^{-\alpha} \left(\frac{\left(\frac{r}{r_0}\right)^\alpha}{\alpha} \right)^{-(\alpha+3)/2\alpha}$$

$$\times \exp\left(-\frac{\left(\frac{r}{r_0}\right)^\alpha}{\alpha}\right) \text{Whittaker}M\left(3/\alpha - (\alpha + 3)/2\alpha, (\alpha + 3)/2\alpha + 1/2, \frac{2\left(\frac{r}{r_0}\right)^\alpha}{\alpha}\right)$$

$$\begin{aligned}
& + \left(\frac{1}{3(2\alpha + 3)} \right) \alpha^2 r^3 2^{(3/\alpha - 1 - (\alpha + 3)/2\alpha)} \left(\frac{(r/r_0)^\alpha r^{-\alpha}}{\alpha} \right)^{3/\alpha} (\alpha + 3) (r/r_0)^{-\alpha} \\
& \times \left(\frac{(r/r_0)^\alpha}{\alpha} \right)^{-(\alpha + 3)/2\alpha} \exp\left(-\frac{(r/r_0)^\alpha}{\alpha}\right) WhittakerM\left(3/\alpha - (\alpha + 3)/2\alpha + 1, (\alpha + 3)/2\alpha + 1/2, \frac{2(r/r_0)^\alpha}{\alpha}\right) + C_1
\end{aligned}$$

where the integration constant is chosen as (in order that $b(r_0) = r_0$ is satisfied)

$$\begin{aligned}
C_1 = \frac{-r_0}{6\alpha^2 + 27\alpha + 27} & \left(A\pi r_0^2 \exp(1/\alpha) 2^{(3\alpha - 3)/2\alpha} \alpha^{1 + (\alpha + 3)/2\alpha} \right) \\
& [\alpha(5 + \alpha) WhittakerM(-(\alpha + 3)/2\alpha, (2\alpha + 3)/2\alpha, 2/\alpha) \\
& + (3 + \alpha) WhittakerM((\alpha + 3)/2\alpha, (2\alpha + 3)/2\alpha, 2/\alpha) - 6\alpha - 9].
\end{aligned} \tag{19}$$

Note that in this expression WhittakerM stands for the Whittaker function [1]. The second order differential equation satisfied by $b(r)$ in our present analysis is given by

$$b'' = \frac{2b'}{r} \left[1 - \left(\frac{r}{r_0} \right)^\alpha \right] \tag{20}$$

which follows from Eq.(12). The redshift function $f(r)$ versus radial coordinate r is plotted in Fig.7.

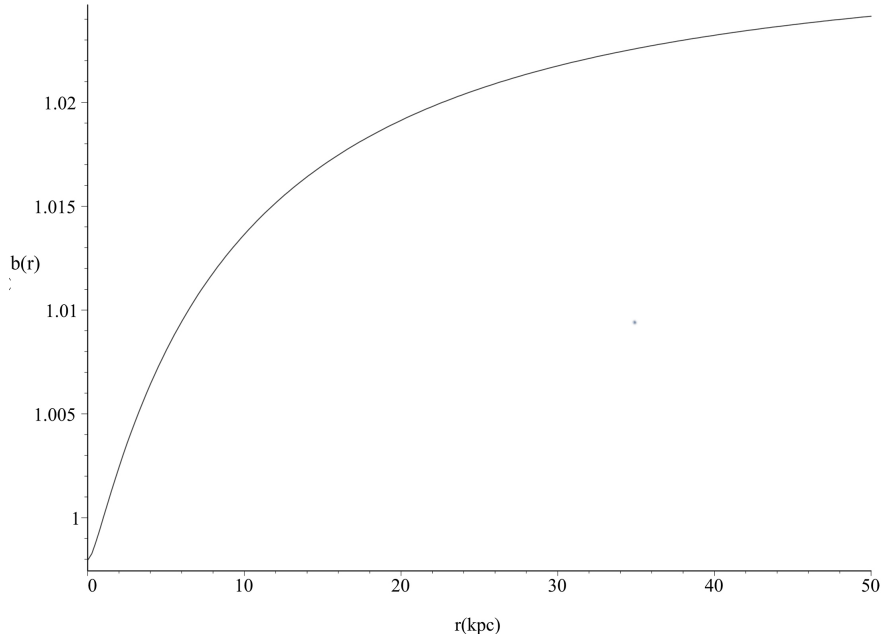


FIG. 8: The shape function b versus radial coordinate r with the parameters $r_0 = 1$ and $\rho_0 = 0.0001$

It can be checked that the wormhole throat condition of $b(r_0) = r_0$ is satisfied. It is shown in Figs. 10 and 11. For the Milky Way galaxy, we have $r_0 = 9.11$ kpc and $\rho_0 = 5 \times 10^{-24} (r_0/8.6 \text{ kpc})^{-1} \text{ g cm}^{-3}$ [4, 32, 42] in order that r_0 is greater than the horizon of the supermassive black hole. This is necessary for the wormhole to be traversable. The choice of r_0 as throat radius can be justified from the fact that r_0 plays the role of the core radius for the galaxy. For this reason we rely on Eq.(4) since for $r > r_0$ there is a turning point for the density distribution. We admit, however, that the exact choice of r_0 as the throat radius, unless a better choice is made, is open to criticism. Furthermore, the flare-out condition ($b' < 1$)

$$b' = 8\pi\rho r^2 = 8\pi r^2 \rho_0 \exp\left[-\frac{2}{\alpha} \left(\left(\frac{r}{r_0} \right)^\alpha - 1 \right)\right] \tag{21}$$

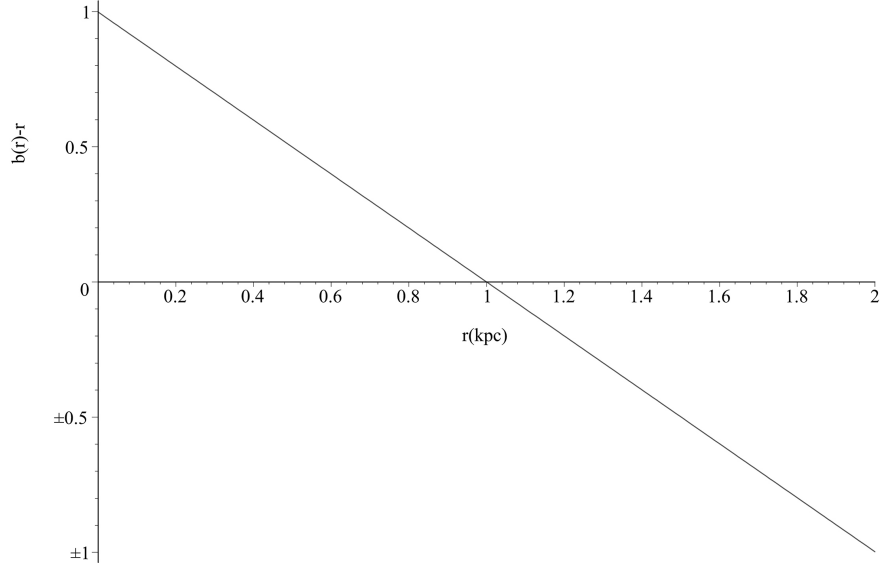


FIG. 9: The radius of the throat is obtained where $b(r)-r$ cuts r axis or the values $r_0 = 1$ and $\rho_0 = 0.0001$

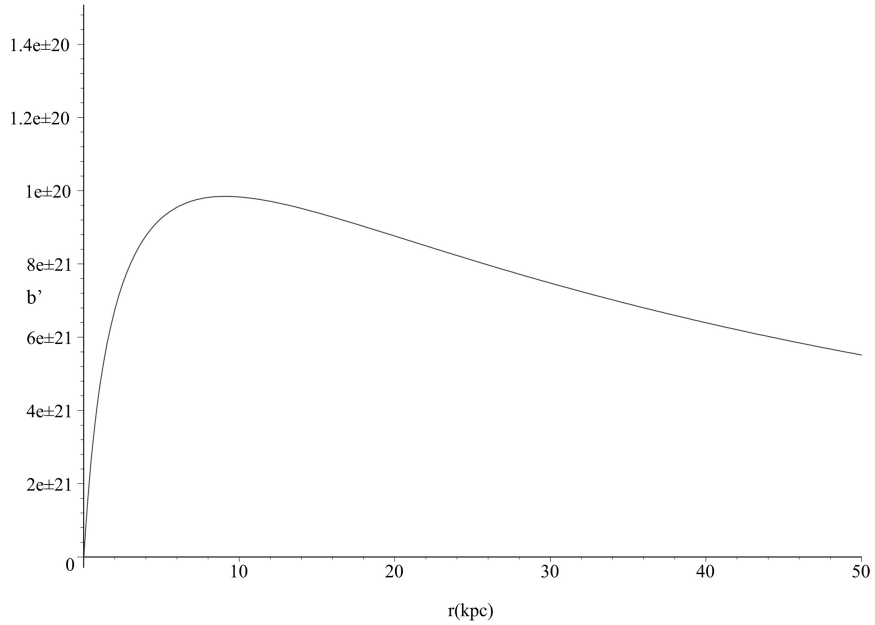


FIG. 10: b' versus r for Milky Way ($r_0 = 9.11$ kpc and $\rho_0 = 5 \times 10^{-24} (r_0/8.6 \text{ kpc})^{-1} \text{ g cm}^{-3}$ [4, 32, 42])

is also satisfied for the Milky Way galaxy $b'(r_0) = 0.98 \times 10^{-20} < 1$ (Fig.10) and also all spherical stellar systems as shown in Fig. 11. In addition, both the star-count and kinematic data of the Milky Way stellar halo are well-represented by an Einasto profile with index $\alpha \approx 0.5$ and effective radius ≈ 20 kpc, if the dark halo has a flat rotation curve (Figs. 4 and 5) [15].

Finally, for the sake of completeness the radial and lateral pressures are calculated easily from Eqs.(8-14) as

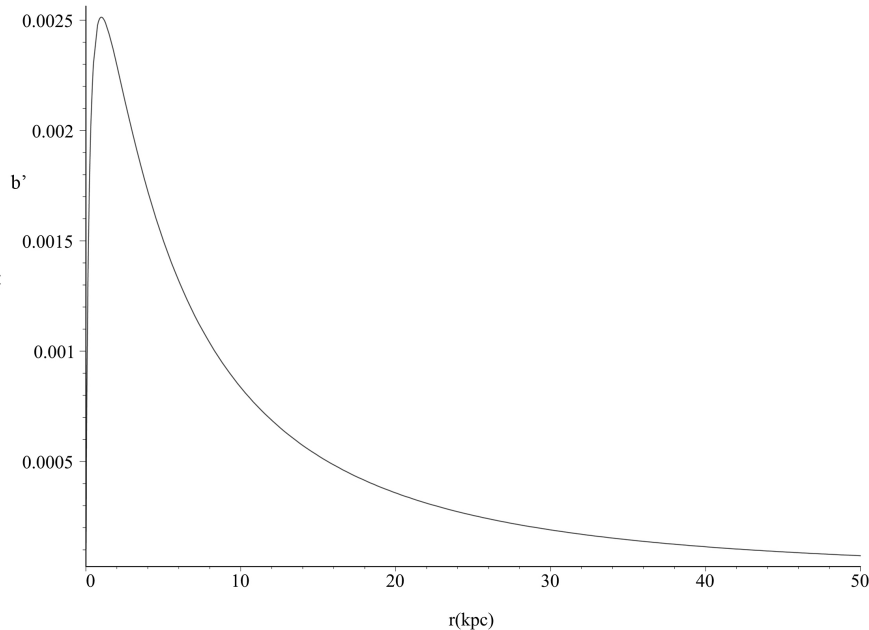


FIG. 11: b' versus r ($r_0 = 1$ and $\rho_0 = 0.0001$)

$$p_r = \frac{1}{8\pi} \left(\frac{-b}{r^3} + 2\left(1 - \frac{b}{r}\right) \frac{f'}{r} \right), \quad (22)$$

$$p_t = \frac{1}{8\pi} \left\{ \left(1 - \frac{b}{r}\right) \left[f'' + f'^2 + \frac{f'}{r} - \left(f' + \frac{1}{r}\right) \left(\frac{b'r - b}{2r(r-b)}\right) \right] \right\} \quad (23)$$

in which $f(r)$ and $b(r)$ are to be substituted from the solution (Eqns. 17- 19).

Note that the null energy condition ($\rho + p_r < 0$) is violated so that the flare-out condition for a wormhole is satisfied according to Fig. 12. Let us note also that those pressures have not been used in the present study but it can be anticipated that for a future stability analysis they will be needed.

III. CONCLUSION

Existence of traversable wormholes is an important problem in physics both at micro and macro scales. There is no doubt that together with black holes wormholes constitute the most interesting objects in our entire universe. On the one hand collision of ultra-energetic particles may create these objects while at the other extreme they form naturally in galactic systems of cosmic dynamics. Once formed, in order to survive traversable wormholes must satisfy certain criteria of stability, otherwise they will decay instantly into more stable objects. Besides stability energy conditions are also of prime importance concerning traversable wormholes. This demands negative energy density which is not available in classical physics although there are rooms for it in the quantum domain. Let us add also that a recent trend is to modify the geometry of throats and obtain thin-shell wormholes [22, 43] supported by positive total energy, for this see [33, 34] and references cited therein. However, the minimum requirement of violating null-energy condition (NEC) provides that $\rho + p_r < 0$, without specifying the (-) condition for the energy density. As a matter of fact NEC provides us a jumping board into the realm of traversable wormholes. Stability, on the other hand, admittedly and for completely technical reasons remains open in our present study. This item may be considered as a separate subject in our future analysis.

This work is motivated mainly by Ref. [50], which discusses the possible formation/existence of traversable wormholes in our own galaxy, Milky Way. Their conclusion that traversable wormholes may exist both at the inner and outer parts of our spiral galaxy has been revised by using a different density distribution. Namely, we adapt the Einasto

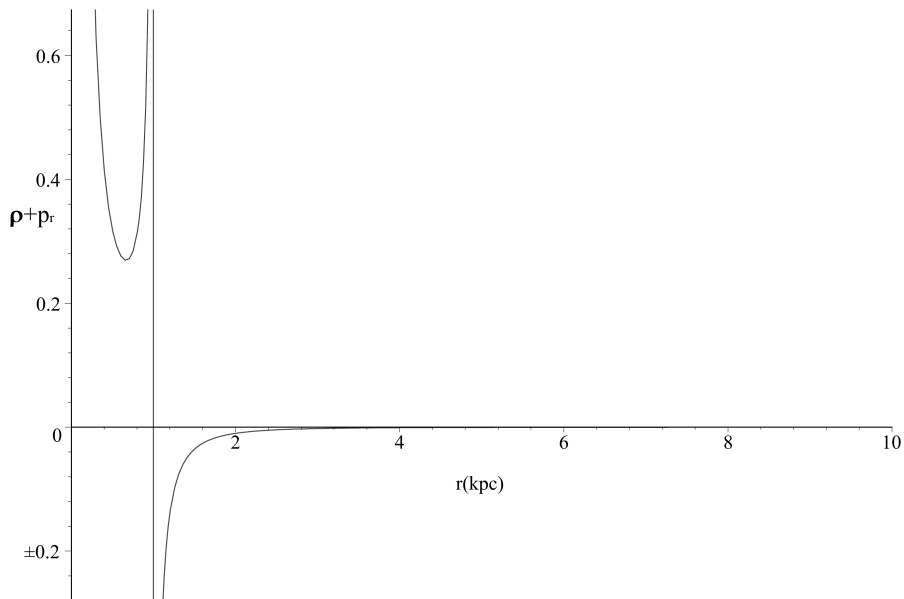


FIG. 12: Null energy condition ($\rho + p_r < 0$) for the values of parameters $r_0 = 1$ and $\rho_0 = 0.0001$

density profile [12, 13] which differs much from the Navarro- Frenk- White (NFW) profile employed in [41, 50]. Our analysis suggests accordingly that at the central region since the NEC is not violated, we do not get any traversable wormholes. This explains also the choice of the throat outside of the central region. Yet at the outer regions, the NEC is violated so that the flare-out condition for traversable wormhole is satisfied and we expect formation of traversable wormholes. This result is not specific to Milky Way alone but is valid for any spiral galaxy once it obeys a mass distribution given by Einasto profile. It is worthwhile therefore to check other mass distributions and see the resulting consequences. In conclusion we wish to comment that the DM lurking in the innermost part of the Milky Way [24], may support the existence of traversable wormholes that contains our solar system as well.

IV. ACKNOWLEDGMENT

We would like to thank the anonymous reviewers for their useful comments and suggestions which helped us to improve the paper.

-
- [1] Abramowitz M.,Stegun I. A. (Eds.), (1972) Handbook of Mathematical Functions with Formulas, Graphs, and Mathematical Tables, 9th printing. New York: Dover
 - [2] Bernal N. & Palomares-Ruiz S.,(2012), JCAP, **01**, 006
 - [3] Bozorgnia N. et al., (2013), JCAP, **1312**, 050
 - [4] Castignani G., Frusciante N., Vernieri D. & Salucci P., (2012), Nat. Sci. **4**, 265
 - [5] Chandrasekhar S., (1983), Mathematical Theory of Black Holes (Oxford Classic Texts)
 - [6] Chan T.K., et al., (2015), MNRAS, **454**, 3, 2981-3001
 - [7] Cui Y., (2015), Mod. Phys. Lett. A, **30**, 37, 1530028
 - [8] Cline D.B., (2016), Phys.Scripta, **91**, no.3, 033008
 - [9] Dhar B.K. & Williams L.L.R., (2010), MNRAS, **405** (1), 340
 - [10] Dutton A.A. & Maccio A.V., (2014),MNRAS, **441** (4), 3359
 - [11] Duffy A.R., et al., (2010),MNRAS, **405**, 4, 2161-2178
 - [12] Einasto J.,(1965),Trudy Inst. Astrofiz. Alma-Ata, **5**, 87
 - [13] Einasto J. & Haud U., (1989), Galaxy Astron. Astrophys., **223**, 89
 - [14] Einstein A. & Rosen N., (1935), Phys. Rev., **48**, 73-77
 - [15] Evans N.W. & Williams A.A., (2014), MNRAS,**443** (1), 791
 - [16] Fan J., Katz A., Randall L., Reece M. & Williams A.A., (2013), Phys.Dark Univ. **2**, 139-156

- [17] Fan J., Katz A., Randall L. & Reece M., (2013), *Phys.Rev.Lett.* **110**, no.21, 211302
- [18] Flamm L., (1916), *Phys.Z.* **17**, 448
- [19] Foot R. & Vagnozzi S., (2015), *Phys.Rev. D* **91**, 023512
- [20] Garrett K., Duda G & Williams A.A., (2011), *Adv.Astron.* **2011**, 968283
- [21] Gaskins J.M., (2016), arXiv:1604.00014
- [22] Halilsoy M., Ovgun A. & Mazharimousavi S.H., (2014), *Eur.Phys.J. C* **74**, 2796
- [23] Hjorth J., Williams L.L.R., Wojtak R. & McLaughlin M., arXiv:1508.02195
- [24] Iocco F., M. Pato & G. Bertone, (2015), *Nature Physics*, **11**, 245
- [25] Jeffreys H. & Jeffreys B. S., (1988), "The Exponential and Related Integrals." §15.09 in *Methods of Mathematical Physics*, 3rd ed Cambridge, England: Cambridge University Press, pp. 470-472
- [26] Kirillov A.A., Savelova E.P., (2015), arXiv:1512.01450
- [27] Kuhfittig P.K.F., (2014), *Eur.Phys.J.C*, **74**, 2818
- [28] Kuhfittig P.K.F., (2014), *Fund.J.Mod.Phys.* **7**, 111-119
- [29] Kuhfittig P.K.F., (2015), *Int.J.Mod.Phys. D* **24**, no.03, 1550023
- [30] Landau L.D. & Lifshitz E.M., (1975), *The Classical Theory of Fields* (Oxford, Pergamon Press)
- [31] Lovell M.R., Frenk C.S., et al., (2014), *MNRAS*, **439**, (1), 300
- [32] Maccio A.V., et al., (2012), *APJL*, **744**, L9
- [33] Mazharimousavi S.H. & Halilsoy M., (2015), *Eur.Phys.J. C*, **75**, 6, 271
- [34] Mazharimousavi S.H. & Halilsoy M., (2015), *Eur.Phys.J. C*, **75**, no.2, 81
- [35] Merritt D., Graham A., et al., (2006), *AJ*, **132**, 6, 2685
- [36] Morris M.S. & Thorne K.S., (1988), *Am. J. Phys.*, **56**, 395
- [37] Morris M.S., Thorne K.S. & Yurtsever U., (1988), *Phys.Rev.Lett.* **61**, 1446-1449
- [38] Myrzakulov R., Sebastiani L., Vagnozzi S. & Zerbini S., (2015), arXiv:1510.02284
- [39] Nandi K.K., Filippov A.I., Rahaman F., et al., (2009), *MNRAS*, **399**, 2079
- [40] Narikawa T. & Yamamoto K., (2012), *JCAP*, **05**, 016
- [41] Navarro J.F., Frenk C.S. & White S.D.M., (1996), *APJ*, **462**, 563
- [42] Nesti F. & Salucci P., (2013), *MNRAS*, **7**, 16
- [43] Ovgun A. & Sakalli I., arXiv:1507.03949
- [44] Pato M. & Iocco F., (2015), *APJ*, **803**, L3
- [45] Pato M., Iocco F. & Bertone G., *JCAP* **1512**, no.12, 001
- [46] Planck Collaboration, P. A. R. Ade et al., (2014), *Astron. Astrophys.* **571**, A20
- [47] Poisson E. & Visser M., (1955), *Phys.Rev. D* **52**, 7318-7321
- [48] Rahaman F., Kalam M., De Benedictis A., Usmani A.A. & Ray S., (2008), *MNRAS*, **27**, 389
- [49] Rahaman F., Kuhfittig P.K.F., Ray S. & Islam N., (2014), *Eur. Phys. J. C*, **74**, 2750
- [50] Rahaman F., Salucci P., Kuhfittig P.K.F., Ray S. & Rahaman M., (2014), *Annals of Phys.*, **350**, 561-567
- [51] Rahaman F., Shit G.C., Sen B. & Ray S., (2016), *Astrophys Space Sci*, **361**, 1, 37
- [52] Rahaman F., Sen B., Chakraborty K. & Shit G.C., (2016), *Astrophys.Space Sci.* **361**, no.3, 90
- [53] Retana-Montenegro E., et al., (2012), *A&A* **540**, A 70
- [54] Rocha M., et al., (2013), *MNRAS* **430**, 1, 81-104
- [55] Salvador-Sole E., Vinas J., Manrique A. & Serra S., (2012), *MNRAS*, **423** (3), 2190
- [56] Siutsou I., Arguelles C.R. & Ruffini R., (2015), *Astronomy Reports* **59**, 7, 656
- [57] Umetsu K., Zitrin A., et al., arXiv:1507.04385
- [58] Wheeler J., (1955), *Phys. Rev.*, **97**, 511-536
- [59] Vera R.C., Kent F.W., (1970), *The Astrophysical Journal* **159**, 379.
- [60] Vera-Ciro C.A., Helmi A., Starkenburg E. & Breddels M.A., (2013), *MNRAS*, **428** (2), 1696
- [61] Visser M., (1989), *Phys.Rev. D* **39**, 3182-3184
- [62] Visser M., (1989), *Nucl.Phys. B* **328**, 203-212
- [63] Visser M., Kar S., Dadhich N., (2003), *Phys.Rev.Lett.* **90** 201102
- [64] Vogelsberger M., Zavala J. & Loeb A., (2012), *MNRAS*, **423**, 4, 3740-3752
- [65] Zwicky F., (1933), *Helvetica Physica Acta* **6**, 110-127